

Electronic Supporting Information (ESI):

One-pot synthesis of luminol-gallium nanoassemblies and their peroxidase-mimetic activity for colorimetric detection of pyrophosphate

Xue Tian,^a Wenjing Qi,^{*a} Maoyu Zhao,^a Jianping Lai,^b Di Wu,^a Lianzhe Hu,^a Yan Zhang^a

^a Chongqing Key Laboratory of Green Synthesis and Applications, College of Chemistry,

Chongqing Normal University, Chongqing 401331, P. R. China.

^b Key Laboratory of Eco-Chemical Engineering, Taishan Scholar Advantage and Characteristic Discipline Team of Eco-Chemical Process and Technology, College of Chemistry and Molecular Engineering, Qingdao University of Science and Technology, Qingdao 266042, P. R. China

*Corresponding author. E-mail: wenjingqi616@cqnu.edu.cn (W. Qi); Tel:+86-23-65362777.

Optimization of Method.

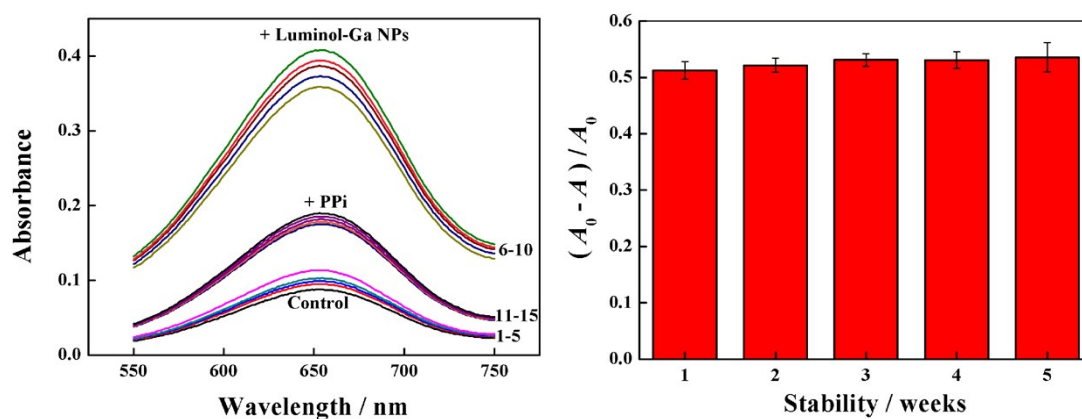


Fig. S1 The stability for catalyst activity of luminol-Ga nanoassemblies and its application in PPI detection. $c(\text{PPI}, \mu\text{M})$: 10. $c(\text{luminol}, \text{mM})$: 0.8; $c(\text{Ga}^{3+})$: 0.1 mM; $c(\text{H}_2\text{O}_2, \text{M})$: 0.2; $c(\text{TMB}, \text{mM})$: 1; 0.04 M acetate buffer solution: pH 4.0. A_0 represents the absorbance of luminol-Ga nanoassemblies-TMB- H_2O_2 system (control); A represents the absorbance of luminol-Ga nanoassemblies-TMB- H_2O_2 system in the presence of PPI; $(A_0 - A)/A_0$ represents the absorbance decreased effect after the addition of PPI to luminol-Ga nanoassemblies-TMB- H_2O_2 system. All the error bars represent the standard deviation of three measurements.

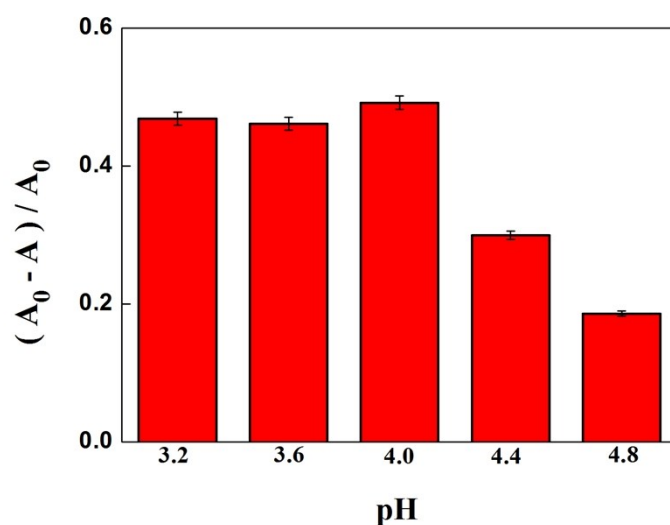


Fig. S2 The effect of pH on the PPI detection. 0.04 M acetate buffer solution pH: 3.2, 3.6, 4.0, 4.4 and 4.8. $c(\text{PPI}, \mu\text{M})$: 15; $c(\text{luminol}, \text{mM})$: 0.8; $c(\text{Ga}^{3+})$: 0.1 mM; $c(\text{H}_2\text{O}_2, \text{M})$: 0.2; $c(\text{TMB}, \text{mM})$: 1; 0.04 M acetate buffer solution: pH 4.0. A_0 represents the absorbance of luminol-Ga nanoassemblies-TMB- H_2O_2 system (control); A represents the absorbance of luminol-Ga nanoassemblies-TMB- H_2O_2 system in the presence of PPI; $(A_0 - A) / A_0$ represents the absorbance decreased effect after the addition of PPI to luminol-Ga nanoassemblies-TMB- H_2O_2 system. All the error bars represent the standard deviation of three measurements.

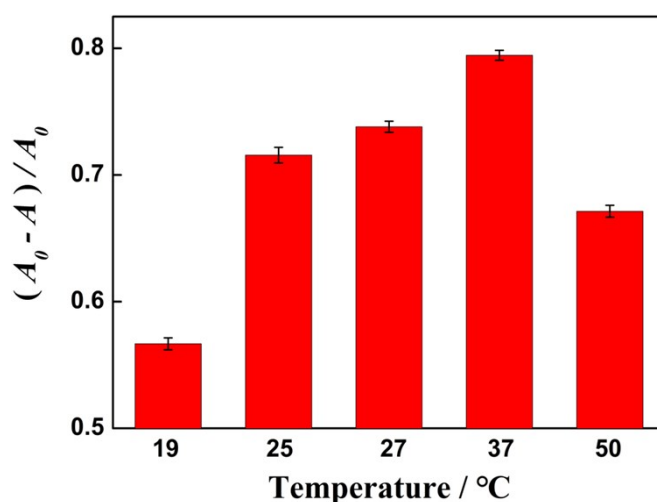


Fig. S3 The effect of oxidation reaction temperature on PPI detection using luminol- Ga^{3+} nanoassemblies. Temperature ($^{\circ}\text{C}$): 19, 25, 27, 37 and 50. $c(\text{PPI}, \mu\text{M})$: 15;

$c(\text{luminol, mM})$: 0.8; $c(\text{Ga}^{3+})$: 0.1 mM; $c(\text{H}_2\text{O}_2, \text{M})$: 0.2; $c(\text{TMB, mM})$: 1; 0.04 M acetate buffer solution: pH 4.0. A_0 represents the absorbance of luminol-Ga nanoassemblies-TMB- H_2O_2 system (control); A represents the absorbance of luminol-Ga nanoassemblies-TMB- H_2O_2 system in the presence of PPI; $(A_0-A)/A_0$ represents the absorbance decreased effect after the addition of PPI to luminol-Ga nanoassemblies-TMB- H_2O_2 system. All the error bars represent the standard deviation of three measurements.

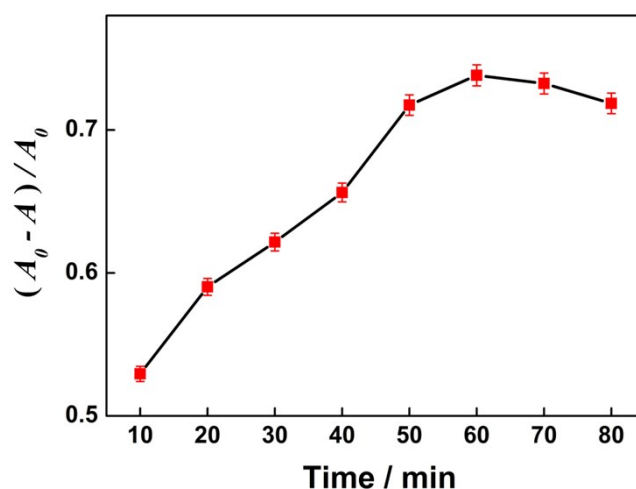


Fig. S4 The effect of oxidation reaction time on PPI detection using luminol- Ga^{3+} nanoassemblies. Reaction time (min): 10, 20, 30, 40, 50, 60, 70 and 80. $c(\text{PPI, } \mu\text{M})$: 15; $c(\text{luminol, mM})$: 0.8; $c(\text{Ga}^{3+})$: 0.1 mM; $c(\text{H}_2\text{O}_2, \text{M})$: 0.2; $c(\text{TMB, mM})$: 1; 0.04 M acetate buffer solution: pH 4.0. All the error bars represent the standard deviation of three measurements. A_0 represents the absorbance of luminol-Ga nanoassemblies-TMB- H_2O_2 system (control); A represents the absorbance of luminol-Ga nanoassemblies-TMB- H_2O_2 system in the presence of PPI; $(A_0-A)/A_0$ represents the absorbance decreased effect after the addition of PPI to luminol-Ga nanoassemblies-TMB- H_2O_2 system. All the error bars represent the standard deviation of three measurements.

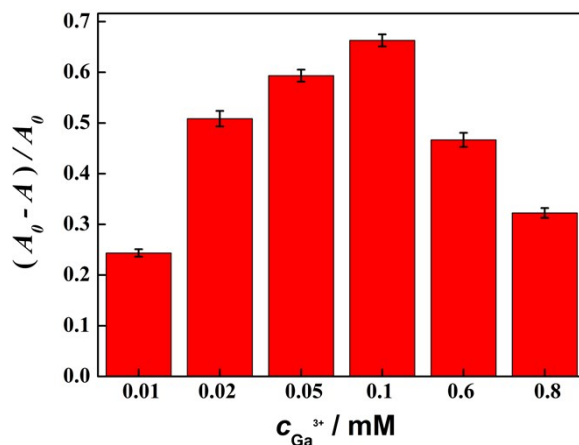


Fig. S5 The effect of Ga^{3+} on PPI detection using luminol- Ga^{3+} nanoassemblies. $c(\text{Ga}^{3+}, \text{mM})$: 0.01, 0.02, 0.05, 0.1, 0.6 and 0.8; $c(\text{luminol}, \text{mM})$: 0.8; $c(\text{PPI}, \mu\text{M})$: 15; $c(\text{H}_2\text{O}_2, \text{M})$: 0.2; $c(\text{TMB}, \text{mM})$: 1; 0.04 M acetate buffer solution: pH 4.0. All the error bars represent the standard deviation of three measurements.

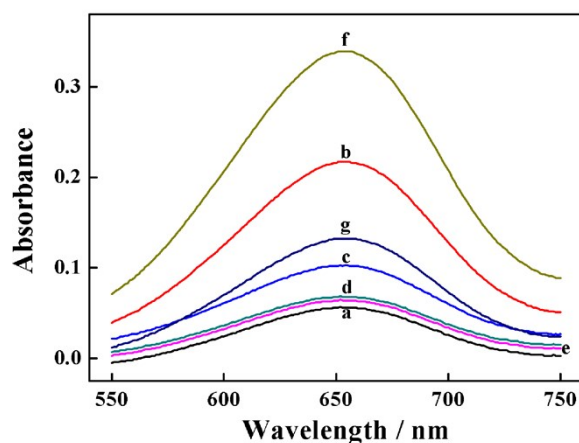


Fig. S6 Comparison of PPI detection and mechanism investigation. TMB- H_2O_2 system (curve a); luminol-TMB- H_2O_2 system (curve b); PPI-luminol-TMB- H_2O_2 system (curve c); Ga^{3+} -TMB- H_2O_2 system (curve d); PPI- Ga^{3+} -TMB- H_2O_2 system (curve e); luminol-Ga nanoassemblies-TMB- H_2O_2 system (curve f); PPI-luminol-Ga nanoassemblies-TMB- H_2O_2 system (curve g). $c(\text{PPI}, \mu\text{M})$: 10; $c(\text{luminol}, \text{mM})$: 0.8; $c(\text{Ga}^{3+})$: 0.1 mM; $c(\text{H}_2\text{O}_2, \text{M})$: 0.2; $c(\text{TMB}, \text{mM})$: 1; 0.04 M acetate buffer solution: pH 4.0.

Table S1 The anti-interference ability.

Coexisting substances	Coexisting concentration (μM)	Changes of absorbance (%)
Na(I), Cl^-	750	+ 2.8
K(I), Cl^-	750	- 3.4
Mg(II), Cl^-	750	+ 3.8
Ca(II), Cl^-	750	- 4.2
Zn(II), SO_4^{2-}	750	- 3.7
Fe(III), Cl^-	750	- 2.8
K(I), NO_3^-	750	+ 2.5
Na(III), PO_4^{3-}	300	+ 4.4
Na(III), HPO_4^{2-}	300	+ 2.8
Na(III), H_2PO_4^-	300	+ 3.2
K(I), I^-	750	- 2.6
K(I), Br^-	750	- 2.9

The concentration of PPI is 15 μM . Other conditions are kept the same with the procedures of PPI detection mentioned above.

Table S2 Recovery tests of PPI in lake water and tap water samples

Samples	Added PPI (μM)	Found PPI (μM, n=3)	Mean recovery (%, n=3)
1 ^a	2	1.97, 1.94, 2.03	98.7 \pm 2.5
2 ^a	6	5.86, 5.92, 5.90	98.2 \pm 0.5
3 ^a	10	10.35, 10.28, 10.16	102.6 \pm 0.9
4 ^b	2	1.91, 1.95, 1.98	97.3 \pm 1.8
5 ^b	6	5.88, 6.21, 6.14	101.3 \pm 2.9
6 ^b	10	9.85, 10.22, 10.10	100.6 \pm 0.2

^a lake water samples ^b tap water samples